DTU Library

Towards a table-top synchrotron based on supercontinuum generation

Petersen, Christian Rosenberg; Moselund, Peter M.; Huot, Laurent; Hooper, Lucy ; Bang, Ole

Published in:
Infrared Physics & Technology

Link to article, DOI:
10.1016/j.infrared.2018.04.008

Publication date:
2018

Document Version
Publisher's PDF, also known as Version of record

Infrared Physics & Technology 91 (2018) 182–186

Contents lists available at ScienceDirect

Infrared Physics & Technology

journal homepage: www.elsevier.com/locate/infrared

Regular article

Towards a table-top synchrotron based on supercontinuum generation

Christian R. Petersen [a,*], Peter M. Moselund [b], Laurent Huot [a,b], Lucy Hooper [b], Ole Bang [a,b]

[a] DTU Fotonik, Technical University of Denmark, 2800 Kgs. Lyngby, Denmark
[b] NKT Photonics, Blokken 84, 3460 Birkerød, Denmark

HIGHLIGHTS

- Direct comparison of synchrotron and supercontinuum brightness from visible to mid-infrared.
- Experimental demonstration of microspectroscopy using a mid-IR supercontinuum source at 6.5 μm.
- Experimental demonstration of supercontinuum transmission spectroscopy from 2.85 μm to 7.69 μm.

ARTICLE INFO

Article history:
Received 16 February 2018
Revised 16 April 2018
Accepted 16 April 2018
Available online 18 April 2018

ABSTRACT

Recently, high brightness and broadband supercontinuum (SC) sources reaching far into the infrared (IR) have emerged with the potential to rival traditional broadband sources of IR radiation. Here, the brightness of these IR SC sources is compared with that of synchrotron IR beamlines and SiC thermal emitters (Globars). It is found that SC sources can deliver a brightness that is 5–6 orders of magnitude higher than Globars and 1–2 orders of magnitude higher than typical IR beamlines, matching the beamlines at least out to 10.6 μm (940 cm^{-1}). This means that these sources can now cover nearly all of the 800–5000 cm^{-1} spectrum (2–12.5 μm) which is frequently used in IR spectroscopy and microscopy. To demonstrate applicability, such an IR SC source was used for transmission spectroscopy of highly scattering filtration membranes from 3500 to 1300 cm^{-1}, and transmission microscopy of colon tissue at 1538 cm^{-1}.

The high brightness beamlines of synchrotrons have over the past decades enabled an astounding range of measurements covering the entire spectrum from hard X-ray to microwaves in diverse fields varying from bio-medicine, geology, and material science to forensics, art, and archaeometry. In the IR region the combination of high signal to noise ratio (SNR) and diffraction limited beam quality has enabled higher resolution and faster acquisition time for Fourier transform IR (FTIR) imaging and microspectroscopy [1–3], which among other applications has the potential to complement conventional histopathology in the diagnosis of cancer [4]. However, while the number of IR beamlines continues to increase, their availability, flexibility, and operational costs have so far limited widespread use. The cost of establishing a synchrotron radiation facility is in the range of hundreds of millions of euros, and while IR beamlines are typically one of the least expensive beamlines in synchrotron facilities the price of establishing such a beamline in an existing facility has been estimated to be on the order of three million euros and requiring half a million euros in annual upkeep [5]. For many applications IR beamlines has therefore served mainly as proof-of-concept workstations for demonstrating advanced techniques that are otherwise inaccessible using traditional thermal light sources.

For a large part of the mid-IR spectrum this is now changing with the development of new compact SC sources based on optical fibers and high power lasers. In comparison, a turnkey long-wavelength mid-IR SC source, similar to the ones that are already commercially available in the short-wavelength mid-IR, will soon be able to provide a two orders of magnitude brighter beam from a portable turn-key package at a price two orders of magnitude less than a beamline and without requiring access to an already established synchrotron facility. Fig. 1 illustrates the main features and differences between SC sources, synchrotron beamlines, and thermal light sources. Fiber-based SC sources are broadband light sources based on extreme spectral broadening of high intensity pump laser pulses through a cascade of nonlinear processes in specially designed optical fibers [6]. Such sources have been available in the visible and near-IR for over a decade, where they have become the excitation light source of choice for a number of advanced microscopy techniques, such as multiphoton- and stimulated emission depletion (STED) microscopy [7,8]. In the past five years there has been an increasing interest in developing longer wavelength SC sources to enable applications in the mid-IR, and now sources extending to 4 μm have become commercially

* Corresponding author.
E-mail address: chru@fotonik.dtu.dk (C.R. Petersen).

https://doi.org/10.1016/j.infrared.2018.04.008
1350-4495/

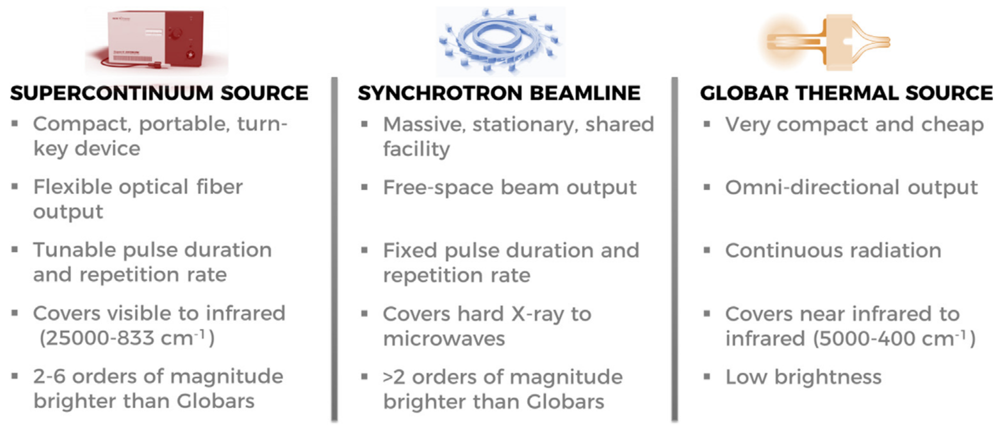

Fig. 1. Brief comparison between features of SC sources, synchrotron beamlines, and Globars.

available (NKT Photonics, Le Verre Fluoré, Novae, NP Photonics, Alphanov, Leukos), and in some cases up to 4.7 μm (2128 cm^{-1}) [9,10]. However, most IR applications require a source that can cover most of the fingerprint region (1500–500 cm^{-1}/6.7–20 μm) containing highly distinctive absorption features from the fundamental vibrational resonances of molecules.

Therefore, there has been a strong push in the academic community to reach even further into the mid-IR and consequently broad spectra reaching beyond 13 μm has been demonstrated [11–13]. Initially, these demonstrations were performed using large femtosecond laser beamlines with low repetition rate and average power, but with recent advances in the design of optical fibers and pump lasers SC sources with high quality beam profiles, high average power levels, and compact footprints are now emerging [14–17]. While such sources cannot cover THz applications they span almost the entire 800–5000 cm^{-1} region that is most commonly applied in mid-IR spectroscopy, and can as such be considered for a wide range of IR applications as a "table-top synchrotron beamline". These sources should make it possible for many of the measurement techniques, which have previously been confined to IR beamlines, to gain more widespread application. For example, in a recent demonstration such a fiber-coupled SC source was used for mid-IR microspectroscopy of tissue in the 5.7–7.3 μm (1370–1754 cm^{-1}) wavelength range [18].

However, while the concept of a table-top synchrotron beamline is exciting, it comes with significant challenges. Unlike synchrotron radiation, which is generated in free-space from e.g. a bending magnet accelerator, SC radiation is generated within a nonlinear medium – in this case an optical fiber. The need for a nonlinear medium imposes several limitations on a SC system, such as a maximum pump power, output power, and bandwidth enforced by the damage threshold, loss and transparent bandwidth

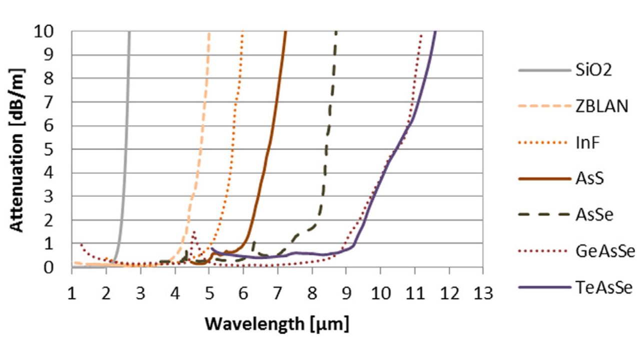

Fig. 2. Attenuation of mid-IR fibers made from various materials as reported in the literature.

of the medium, respectively. Optical fibers are typically fabricated from high purity glasses, which means that the bandwidth of the fiber depends mainly on the electronic and molecular resonances of the host glass. Fig. 2 present the power attenuation coefficient in dB/m of optical fibers fabricated from different glasses, which provides a general guideline for the maximum wavelengths that can be reached using such fibers.

SC sources based on silica and other oxide glass fibers are generally limited to around 2.4 μm, whereas fluoride glasses, such as ZrF4-BaF2-LaF3-AlF3-NaF (ZBLAN) and InF_3, are transparent out to 4.7 μm and 5.5 μm, respectively. SC sources based on silica and fluoride fibers have benefitted from the maturity of the fiber- and pump laser technology in the near-IR, which has led to very efficient sources. To extend the spectrum beyond 6 μm, chalcogenide glasses (AsS, AsSe, GeAsSe, TeAsSe) are typically employed, but because the bandgap of these glasses are shifted to allow for long-wavelength transmission, chalcogenide fibers cannot be pumped efficiently by near-IR lasers and thus more exotic pump sources must be used. An example of this is shown in Fig. 3 for a chalcogenide SC source based on a tapered GeAsSe photonic crystal fiber pumped by a free-space optical parametric amplifier (OPA) source operating at 4 μm (see Ref. [15] for details), and similar results have been obtained with early-development mid-IR fiber-based pump sources [14]. Another promising approach to overcoming the limitations of the chalcogenide fibers is to employ so-called cascaded SC in which a near-IR pump is continuously broadened in a series of concatenated fibers, each extending the transmission bandwidth compared to the previous fibers in the cascade. An example of this is a silica fiber-based SC source that is launched first into a fluoride fiber extending the long-wavelength edge from 2.4 μm to 4.5 μm, and subsequently into a chalcogenide fiber extending the spectrum to beyond 6 μm. Such sources have been demonstrated in the lab [16,19,20], and because they are based on mature near-IR pump and fiber technology they have the potential to become compact, portable, and commercially-viable instruments.

One metric for comparing SC sources with traditional sources of broadband IR radiation is the spectral brightness defined as the source intensity per solid angle. The brightness of a synchrotron $B_S(\lambda)$ can be approximated by [3]:

$$B_S(\lambda) = 3.78 \times 10^{20} I \cdot BW/\lambda^2 \quad [\mathrm{ph/s/mm^2/sr}] \tag{1}$$

where I is the stored current of the ring, BW is the normalization bandwidth and λ is the wavelength. By using $I = 0.5$ A and BW = 0.1% the brightness can be determined as function of wavelength, and the result is shown in Fig. 3. We compared this analytic expression for the synchrotron spectral brightness to the brightness

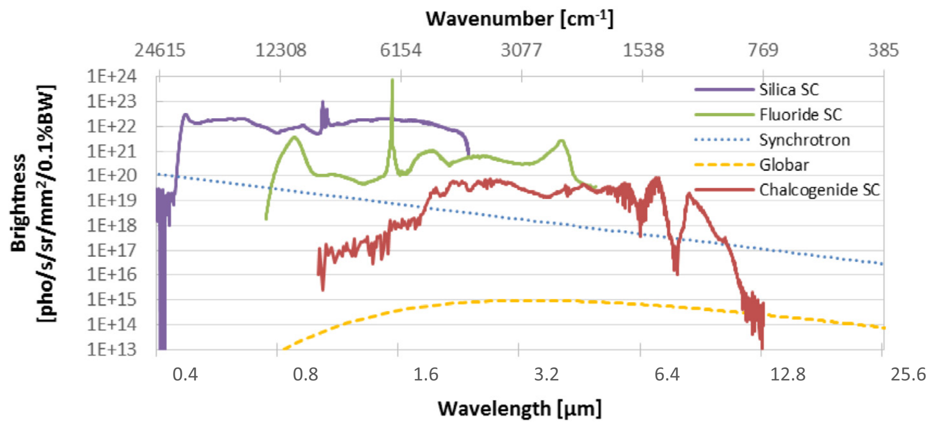

Fig. 3. Brightness of silica, fluoride, and chalcogenide fiber-based SC sources compared to a synchrotron, the sun (5778 K blackbody), and a Globar (1500 K blackbody). The spectral brightness of the synchrotron, Globar, and SC sources were calculated from Eqs. (1)–(3), respectively.

reported for the Diamond [21], NSLS [2], and SLS [22] in the literature and found that the analytic expression was equal to or higher than these. The brightness of a Globar thermal emitter $B_G(\lambda)$ can be estimated from the Planck blackbody radiation formula, resulting in:

$$B_T(\lambda) = \frac{2hc^2}{\lambda}\frac{1}{(e^{hc/k_BT\lambda}-1)E_p} \quad [\mathrm{ph/s/mm^2/sr}] \tag{2}$$

where h is Plancks constant, c is the speed of light, k_B is the Boltzmann constant, T is the blackbody temperature, and E_p is the photon energy. The corresponding brightness of the SC sources $B_{SC}(\lambda)$ was also approximated using the following equation:

$$B_{SC}(\lambda) = \frac{\mathrm{PSD}}{E_\mathrm{p}}\cdot(1[\mathrm{nm}]/0.1\%BW)/(A_\mathrm{eff}\Omega) \quad [\mathrm{ph/s/mm^2/sr}] \tag{3}$$

where PSD is the measured power spectral density, A_{eff} is the effective modal area, and Ω is the solid angle of the output beam. The effective modal area was calculated as a function of wavelength using finite-element modelling based on the refractive indices of the fiber core and cladding glasses, and the solid angle was calculated from $\Omega = 2\pi(1-\cos(\lambda/\pi w_0))$, where w_0 is the effective mode field radius. The spectral data for the silica and fluoride fiber SC was provided by NKT Photonics, and the chalcogenide fiber data is from Ref. [15]. From Fig. 3 it is clear that the SC sources can provide a much higher brightness over a large part of the spectrum. In general, the maturity and efficiency of optical components, fibers and pump lasers is gradually reduced as one moves towards longer wavelengths, which inevitably results in lower brightness of the SC sources, as seen in Fig. 3. Even so, current state-of-the-art SC sources can match the brightness of a synchrotron from visible wavelengths ~420 nm all the way to 10.6 µm, and with continued efforts these sources should continue to expand towards longer wavelengths and higher power.

Another concern is the noise of SC sources, which is expected to be significantly higher than the noise of thermal sources and synchrotron radiation due to the stochastic nature of the nonlinear

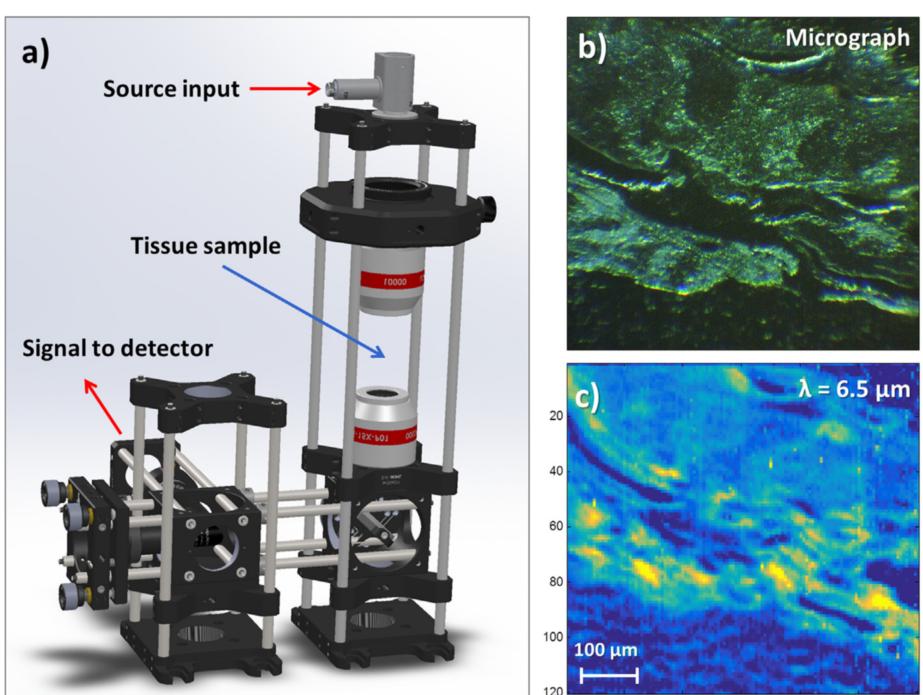

Fig. 4. (a) Fiber-coupled point-mapping microspectroscopy setup. (b) Colon tissue sample micrograph as seen through an optical microscope. (c) Mid-IR SC absorbance map at 6.5 µm wavelength, corresponding to the amide II absorption band.

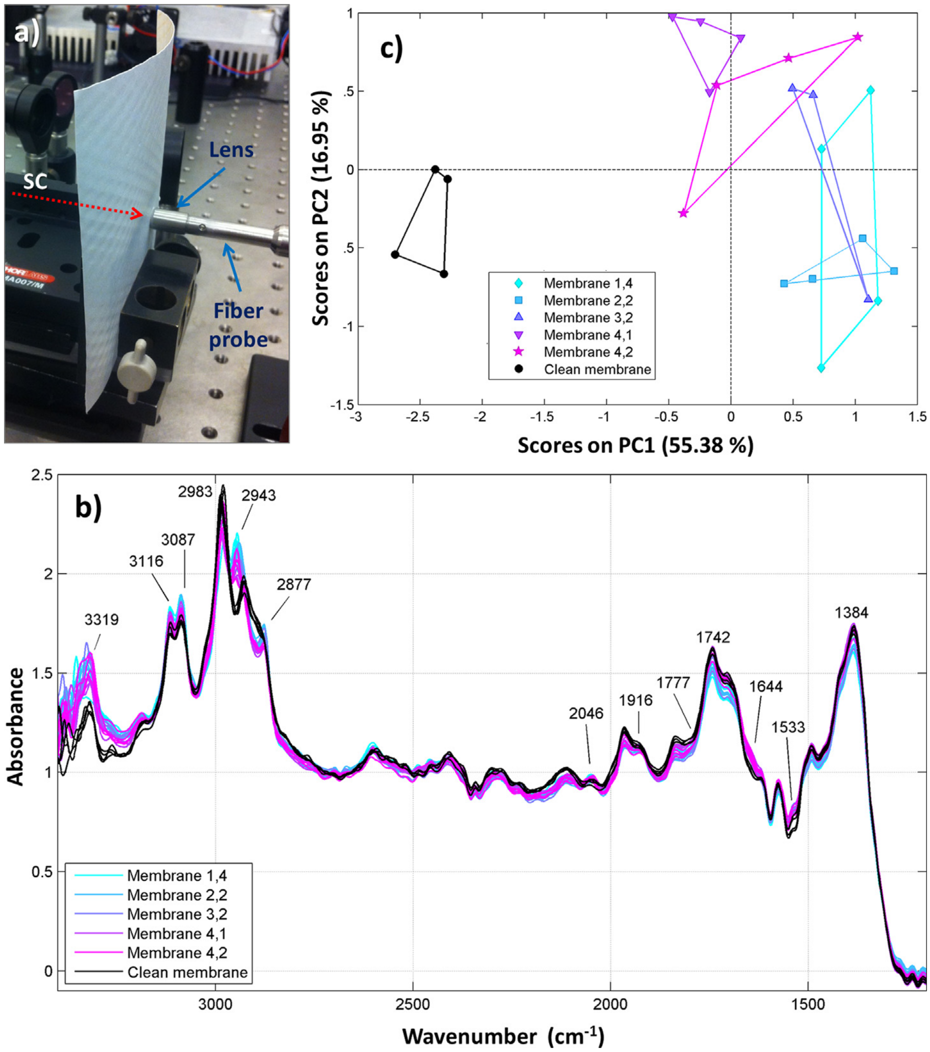

Fig. 5. (a) Transmission spectroscopy of UF membranes using a collimated SC beam and a fiber-coupled FTIR instrument. (b) Absorbance spectra of a clean UF membrane and five fouled UF membranes measured in four different positions. Markers indicate wavenumbers of interest in the following analysis. (c) PCA graph showing clear separation of the clean and fouled membranes, with some overlap between the different fouled samples.

processes involved with spectral broadening. Nonetheless, in a recent demonstration with mid-IR microspectroscopy of liver tissue around 3.5 μm (2857 cm^{-1}) it was found that a SC source could achieve comparable or even higher signal-to-noise ratio (SNR) compared to a synchrotron source [23], enabling shorter acquisition times, which is important for high resolution imaging Fig. 1 show results with IR microspectroscopy of the same parafinized colon tissue sample reported in Ref. [18] using a chalcogenide SC source. The imaging setup shown in Fig. 4(a) was designed for fiber-coupled input and output using reflective optics and objectives to achieve diffraction-limited achromatic performance.

The colon tissue sample, shown in Fig. 4(b) using visible light transmission, was scanned in the beam focus using a piezo-electric translation stage in 5 μm steps, and the transmitted signal was coupled to a grating spectrometer via multimode chalcogenide fiber. The sample was imaged at 6.5 μm (1538 cm^{-1}) which correspond to the amide II absorption band, and the resulting image is shown in Fig. 4(c) highlighting the protein-rich regions of the sample (bright yellow) in contrast to the surrounding connective tissue (light blue[1]).

[1] For interpretation of color in Fig. 4, the reader is referred to the web version of this article.

Another example of where SC sources may be useful is for spectroscopy of highly scattering samples, such as ultrafiltration (UF) membranes. UF membranes are used in the dairy industry to concentrate sweet whey from milk, and as a result the membranes require daily cleaning to maintain the required hygienic standards. This results in a significant loss of water resources, consumption of chemicals, and production down-time [14]. Furthermore, the cleaning procedures only remove the main fouling layers of the membrane, leaving some irreversible residual fouling that eventually requires replacing the membrane. Recently J. Jensen from the Department of Food Science at Copenhagen University (Denmark) investigated residual fouling of UF membranes from the dairy industry, by infrared attenuated total reflectance (ATR) [14]. One issue with ATR is that it is a surface technique, and so to make sure that residual fouling of the deeper membrane layers are also included in the analysis, the membranes must be measured in transmission. However, due to the high absorption and scattering from the membranes, standard FTIR transmission methods was not possible, but with the added brightness and spatial coherence of our SC source a proof-of-concept transmission spectroscopy experiment was performed together with T. Ringsted from the Department of Food Science at Copenhagen University. The membrane was made from poly-ethersulfone (PES), and the five sheets used in this experiment came from different parts of a 1 × 1 m membrane segment. Fig. 5(a) shows the experiment, in which a collimated beam from a chalcogenide SC source was transmitted through the roughly 1 mm thick membrane.

The transmitted signal was collected using a fiber probe, comprising a multimode fiber and coupling lens, and the spectrum was measured using a custom fiber-coupled FOSS FTIR instrument. Fig. 5(b) show absorbance spectra of the five fouled membranes measured in four different places on the membrane, and compare these to the spectrum of a clean membrane. The spectra was included in a principle component analysis (PCA), and the resulting graph in Fig. 5(c) show clear separation of the clean and fouled membranes, with some overlap between the fouled samples.

In conclusion, the brightness of SC sources was considered in the range from visible to mid-IR based on measured data and compared to synchrotron and thermal radiation sources. It is found that current SC sources can match the brightness of a synchrotron from visible all the way to 10.6 μm, and with continued improvements in the maturity and efficiency of mid-IR components and optical fibers these sources will be able to cover all of the 800–5000 cm^{-1} spectral region that is of key importance in mid-IR applications. Furthermore, experimental results with IR microscopy and transmission spectroscopy was demonstrated using a mid-IR SC source, which shows the potential of such sources for enabling broadband techniques in a wavelength region that has otherwise been reserved for synchrotron sources. Consequently, the ability to have a bright and broadband light source available in a compact, portable, turn-key device with flexible beam delivery is expected to have a major impact on applications within mid-IR spectroscopy and microscopy.

Conflict of interest

All authors have declared that they have no conflicting interests associated with this work.

Acknowledgements

The authors acknowledge Tine Ringsted from University of Copenhagen, Department of Food Science, for supplying the UF membranes used in the transmission spectroscopy demonstration. This work was supported by the European Commission through the Framework Seven (FP7) project MINERVA (317803; www.minerva-project.eu) and European Union's Horizon 2020 research and innovation program under grant agreement No. 732968 project FLAIR and under the Photonics21 Photonics Public Private Partnership system. The authors also acknowledge financial support from Innovation Fund Denmark, project Light & Food (J. No. 132-2012-3) and project ShapeOCT (J. No. 4107-00011A).

Declaration of interest

The authors are affiliated with the commercial manufacturer of supercontinuum sources NKT Photonics from which the data for the silica and fluoride sources was obtained.

Appendix A. Supplementary material

Supplementary data associated with this article can be found, in the online version, at https://doi.org/10.1016/j.infrared.2018.04.008.

References

[1] M.J. Nasse, M.J. Walsh, E.C. Mattson, R. Reininger, A. Kajdacsy-Balla, V. Macias, R. Bhargava, C.J. Hirschmugl, High-resolution Fourier-transform infrared chemical imaging with multiple synchrotron beams, Nat. Methods 8 (2011) 413–416.

[2] A. Marcelli, A. Cricenti, W.M. Kwiatek, C. Petibois, Biological applications of synchrotron radiation infrared spectromicroscopy, Biotechnol. Adv. 30 (2012) 1390–1404.

[3] P. Dumas, L. Miller, Biological and biomedical applications of synchrotron infrared microspectroscopy, J. Biol. Phys. 29 (2003) 201–218.

[4] J. Nallala, G.R. Lloyd, M. Hermes, N. Shepherd, N. Stone, Enhanced spectral histology in the colon using high-magnification benchtop FTIR imaging, Vib. Spectrosc. 91 (2017) 83–91.

[5] <www.maxiv.lu.se/accelerators-beamlines/beamlines/projects/ir-beamline/> (April 16, 2018).

[6] J.M. Dudley, G. Genty, S. Coen, Supercontinuum generation in photonic crystal fiber, Rev. Mod. Phys. 78 (2006) 1135–1184.

[7] D. Wildanger, E. Rittweger, L. Kastrup, S.W. Hell, STED microscopy with a supercontinuum laser, Opt. Express 16 (2008) 9614–9621.

[8] H. Tu, Y. Liu, D. Turchinovich, M. Marjanovic, J.K. Lyngsø, J. Lægsgaard, E.J. Chaney, Y. Zhao, S. You, W.L. Wilson, B. Xu, M. Dantus, S.A. Boppart, Stain-free histopathology by programmable supercontinuum pulses, Nat. Photonics 10 (2016) 534–540.

[9] P.M. Moselund, C. Petersen, L. Leick, J.S. Dam, P. Tidemand-Lichtenberg, C. Pedersen, Highly stable, all-fiber, high power ZBLAN supercontinuum source reaching 4.75 μm used for nanosecond mid-IR spectroscopy, in: Advanced Solid-State Lasers Congress, JTh5A.9, 2013.

[10] <https://www.leukos-systems.com/sites/default/files/docs/products/electro_mir_.pdf> (April 16, 2018).

[11] T. Cheng, K. Nagasaka, T.H. Tuan, X. Xue, M. Matsumoto, H. Tezuka, T. Suzuki, Y. Ohishi, Mid-infrared supercontinuum generation spanning 2.0 to 15.1 μm in a chalcogenide step-index fiber, Opt. Lett. 41 (2016) 2117–2120.

[12] C.R. Petersen, U. Møller, I. Kubat, B. Zhou, S. Dupont, J. Ramsay, T. Benson, S. Sujecki, N. Abdel-Moneim, Z. Tang, D. Furniss, A. Seddon, O. Bang, Mid-infrared supercontinuum covering the 1.4–13.3 μm molecular fingerprint region using ultra-high NA chalcogenide step-index fibre, Nat. Photonics 8 (2014) 830–834.

[13] Z. Zhao, B. Wu, X. Wang, Z. Pan, Z. Liu, P. Zhang, X. Shen, Q. Nie, S. Dai, R. Wang, Mid-infrared supercontinuum covering 2.0-16 μm in a low-loss telluride single-mode fiber: mid-infrared supercontinuum covering 2.016 μm in a low-loss telluride single-mode fiber, Laser Photonics Rev. 11 (2017) 1700005.

[14] D.D. Hudson, S. Antipov, L. Li, I. Alamgir, T. Hu, M.E. Amraoui, Y. Messaddeq, M. Rochette, S.D. Jackson, A. Fuerbach, Toward all-fiber supercontinuum spanning the mid-infrared, Optica 4 (2017) 1163–1166.

[15] C.R. Petersen, R.D. Engelsholm, C. Markos, L. Brilland, C. Caillaud, J. Trolès, O. Bang, Increased mid-infrared supercontinuum bandwidth and average power by tapering large-mode-area chalcogenide photonic crystal fibers, Opt. Express 25 (2017) 15336–15347.

[16] R.A. Martinez, G. Plant, K. Guo, B. Janiszewski, M.J. Freeman, R.L. Maynard, M.N. Islam, F.L. Terry, O. Alvarez, F. Chenard, R. Bedford, R. Gibson, A.I. Ifarraguerri, Mid-infrared supercontinuum generation from 1.6 to >11 μm using concatenated step-index fluoride and chalcogenide fibers, Opt. Lett. 43 (2018) 296.

[17] B. Zhang, Y. Yu, C. Zhai, S. Qi, Y. Wang, A. Yang, X. Gai, R. Wang, Z. Yang, B. Luther-Davies, High brightness 2.2-12 μm mid-infrared supercontinuum generation in a nontoxic chalcogenide step-index fiber, J. Am. Ceram. Soc. 99 (2016) 2565–2568.

[18] C.R. Petersen, N. Prtljaga, M.C. Farries, J. Ward, B. Napier, G. Lloyd, J. Nallala, N. Stone, O. Bang, Mid-infrared multispectral tissue imaging using a chalcogenide fiber supercontinuum source, Opt. Lett. 43 (2018) 999–1002.

[19] C.R. Petersen, P.M. Moselund, C. Petersen, U. Møller, O. Bang, Spectral-temporal composition matters when cascading supercontinua into the mid-infrared, Opt. Express 24 (2016) 749–758.

[20] L.-R. Robichaud, V. Fortin, J.-C. Gauthier, S. Châtigny, J.-F. Couillard, J.-L. Delarosbil, R. Vallée, M. Bernier, Compact 3–8 μm supercontinuum generation in low-loss as2se3 step-index fiber, Opt. Lett. 41 (2016) 4605–4608.

[21] G.D. Smith, Infrared microspectroscopy using a synchrotron source for arts-science research, J. Am. Inst. Conserv. 42 (2003) 399–406.

[22] L. Quaroni, J. Schneider, D. Armstrong, J. Wambach, P. Lerch, The infrared beamline at the swiss light source: a tool for chemical microanalysis, CHIMIA 64 (2010) 457.

[23] F. Borondics, M. Jossent, C. Sandt, L. Lavoute, D. Gaponov, A. Hideur, P. Dumas, S. Février, Supercontinuum-based Fourier transform infrared spectromicroscopy, Optica 5 (2018) 378–381.